International Journal of Thermophysics, Vol. 20, No. 4, 1999

Depth-Resolved Surface Thermophysical Property Measurement by Laser-Produced Plasmas[1]

Y. W. Kim[2]

A new laser-based method for real-time *in situ* measurement of thermophysical properties of materials has been developed. It entails production by a high-power laser pulse of a plasma plume from the surface of a condensed-phase specimen and simultaneous measurement of a material's response to the excitation. The specimen may be a solid or in a molten state at high temperatures. It has been shown that the thermal diffusivity can be determined, for instance, from the mass loss due to laser excitation. In one implementation the mass loss is determined from the impulse imparted on the surface by the ablated matter which is measured by an impulse transducer. In this paper, we present a new spectroscopic method for measurement of the mass loss, facilitating *in situ* non-contact measurement of the thermal diffusivity for the first time. An implementation of this method is described, whereby the thermal diffusivity of a complex layered surface is determined as a function of depth with resolutions as small as 13 nm.

KEY WORDS: depth-resolved measurements; laser-produced plasmas; surface thermophysical properties.

1. INTRODUCTION

Rapid heating of a condensed phase surface by a short, high-power laser pulse can launch a dense plasma plume into the ambient atmosphere in a nanosecond time scale. We have shown that it is possible to produce a plasma which is representative of the target surface in elemental composition by tailoring the laser pulse profile [1]. The criterion is to maintain the

[1] Paper presented at the Fifth International Workshop on Subsecond Thermophysics, June 16–19, 1998, Aix-en-Provence, France.

[2] Department of Physics, Lewis Laboratory, Building No. 16, Lehigh University, Bethlehem, Pennsylvania 18015, U.S.A.

0195-928X/99/0700-1313$16.00/0

velocity of the surface erosion by laser heating in pace with the velocity of thermal diffusion into the bulk of the target. Under such conditions, the differences in the rate of evaporation of constituent elemental species are overcome. The rate of evaporation is a strong, species-specific function of temperature, and the evaporation process tends to lower the surface temperature through the expenditure of the heat of evaporation. When an alloy is driven to high temperatures by laser heating according to the criterion, the thickness of the volatile layer is kept to a minimum. All elements in the layer are then evaporated together due to the fast feedback regulation of the surface temperature by expenditures of laser energy in the form of the different elemental heats of formation.

According to our detailed numerical simulation of the process, the criterion has a moderately wide range of validity in terms of the laser heating rate. The surface can be overdriven somewhat without incurring greater mass loss as long as the plasma remains subcritical, i.e., the plasma frequency remains below the frequency of the laser. The surface can be slightly underdriven below the criterion because of the collisional equilibration among elemental species within the heating layer. The criterion can be estimated from approximate values of the optical and thermodynamic properties of the specimen. On the other hand, the criterion can be confirmed spectroscopically. When the criterion has been satisfied, the emission spectrum of the laser-produced plasma plume becomes reproducible from one shot to the next, provided that the size of the laser-excited surface area is larger than the characteristic dimensions of elemental segregations at the surface of the specimen.

For a given laser pulse energy and duration, the mass lost from the surface per laser pulse is governed by the thermal diffusivity of the surface matter, the heats of fusion, and evaporation and the ability of the gas-phase species to move away from the surface by diffusion. In fact, for target specimens placed in a vacuum a relationship has been established for the thickness of the surface layer that has been removed [2]:

$$\theta = CD_{\mathrm{T}}{}^{\alpha} M^{\beta} H_{\mathrm{f}}{}^{\gamma} \tag{1}$$

Here θ denotes the thickness in cm, D_{T} the thermal diffusivity in units of $\mathrm{cm}^2 \cdot \mathrm{s}^{-1}$, M the molar weight, and H_{f} the heat of formation in $\mathrm{J} \cdot \mathrm{g}^{-1}$. $C = 11.07 \pm 0.45$, $\alpha = 0.91 \pm 0.01$, $\beta = -\alpha$, and $\gamma = -1$.

The thickness of the matter that has been removed is related to the mass loss by the mass density. The above relationship can thus be written for the mass loss, instead. The mass loss can be measured by measuring the impulse imparted on the target by the matter being ejected due to laser excitation. In this implementation, a high-sensitivity transducer is built into

the specimen holder. The transducer output is then calibrated by applying known impulses to the target. The overall approach has been utilized successfully both for solid specimens and for molten metallic specimens. A RF-levitator heater was used to create rapidly a molten state on top of a long metallic rod specimen mounted on the holder for the measurements [2, 3].

For certain material specimens whose elemental composition is unknown, this laser-produced plasma method offers an additional distinct advantage. The elemental composition can be measured at the same time while the mass loss measurement is made. The mass density and heats of formation of the specimen can be deduced from the composition. The representative plasma plume can be analyzed by quantitative spectroscopy for elemental composition. As it turns out, the target-representative plasmas, so produced according to the criterion, are highly reproducible. Space- and time-resolved measurements of spectral emissions are carried out during a single eruption of the laser-produced plasma in order to determine the relative elemental abundances in the specimen. It is quite natural then to visualize the possibility of extending this capability to measure the mass loss spectroscopically.

In the present paper, we describe the basic steps we have taken to realize this *in situ*, noncontact method of measuring the thermal diffusivity of a metallic alloy specimen. The approach is quite general so that a wide variety of material composition can be addressed. Of particular interest is the question of unfolding the thermophysical properties of a material surface whose elemental composition is different from that of the bulk and, in fact, changes over a short distance into the bulk. Coatings, segregation during solidification, and corrosions are such examples of structured surfaces. Each pulsed laser heating can be tailored to remove a thin slice of the outer surface layer, and this opens up the possibility of complete characterization of the surface layer. We have been able to examine surface layers as thin as 13 nm at a time by controlling the laser parameters within the bounds of the criterion for composition-representative plasma production.

2. EXPERIMENTAL ARRANGEMENT

The experimental setup consists of a 10-cm-diameter cylindrical target chamber, a Q-switched YAG laser, a spectrograph with a 2-D, gated, intensified array detector, a helium flow loop, and a set of synchronization pulse generators. The laser beam is directed into the target chamber by means of a dichroic beam splitter and focused onto the target specimen through a lens which also serves as the front window of the chamber. The laser power density at the target surface is in the range of 10^9 to 10^{11} $W \cdot cm^{-2}$.

A flow of helium is maintained at 1 atm in order to define the medium into which the laser-produced plasma expands. Also, the helium flow transports the submicron particulates that result from cooling of the plasma plume of the target material out of the chamber. This prevents the premature laser breakdowns in helium, which are often precipitated by the presence of the solid particulates.

The plasma emissions are directed onto the entrance slit of the spectrograph by means of the focusing lens and a second lens in front of the spectrograph. The laser is triggered, and the plasma is produced on command. The spectroscopic detector is gated to collect the wavelength-resolved emissions for the duration of 10.5 μs, starting at the onset of the plasma afterglow period when the emission lines are narrow and well separated. The goal is to fully integrate the emission intensities in the individual detector elements for the lifetime of the plasma afterglow.

Each specimen is mounted on a specimen holder which can be inserted into the chamber from the opposite end from the focusing lens. The specimen can be rotated about the optical axis. The distance to the specimen from the focusing lens is adjustable. Specimens are prepared into rectangular pieces, approximately 1×0.5 cm in size and 0.2 cm in thickness.

For the purpose of mass loss determination, a digital Mettler microbalance is used, having a maximum 2-g capacity and 0.1-μg resolution. The specimen is weighed at the end of each fixed-number laser excitation run in order to track the mass loss. The emission spectrum is obtained at each laser excitation, however. Typically, the mass loss is measured after every 10 laser excitations.

3. DEPTH-RESOLVED MASS LOSS MEASUREMENT

We now present a study of the specimen of galvanized low-alloy steel. In this study, the specimen is placed in helium at 1 atm, not in a vacuum. As a precursor to the investigation, two pure specimens of zinc and iron were compared in terms of their respective mass loss responses to laser excitation under a fixed-laser power condition. We expect that the constant coefficient (C) of the scaling relation [Eq. (1)] will vary according to the ambient gas density. The question is whether the scaling relation holds at elevated ambient gas pressure conditions.

The pure substances responded as follows: the mass loss per laser excitation was found to be 0.53 ± 0.02 μg for zinc and 0.12 ± 0.01 μg for iron. Accounting for the fact that the low-intensity reflectance of zinc is 0.7013 at 1.05 μm and that for iron is 0.644 at 1.03 μm [4], the mass loss ratio becomes 5.24 ± 0.22. The coefficient of thermal conduction is 119 and

83.5 $W \cdot m^{-1} \cdot K^{-1}$ at 273 K for zinc and iron, respectively [4]. Combining these results with the mass densities for solid zinc and iron of 6.92 and 7.86 $g \cdot cm^{-3}$, atomic masses for zinc and iron of 63.37 and 55.85, and specific heats for zinc and iron of 0.401 and 0.449 $J \cdot g^{-1} \cdot K^{-1}$ [4], respectively, we obtain a thermal diffusivity of 0.43 $cm^2 \cdot s^{-1}$ for zinc and 0.24 $cm^2 \cdot s^{-1}$ for iron. From Eq. (1) the expected mass loss ratio can then be calculated, and its value is 5.39. This is in very good agreement with the measured value of 5.24 ± 0.22, demonstrating that the scaling relation can be extended to higher ambient gas pressures.

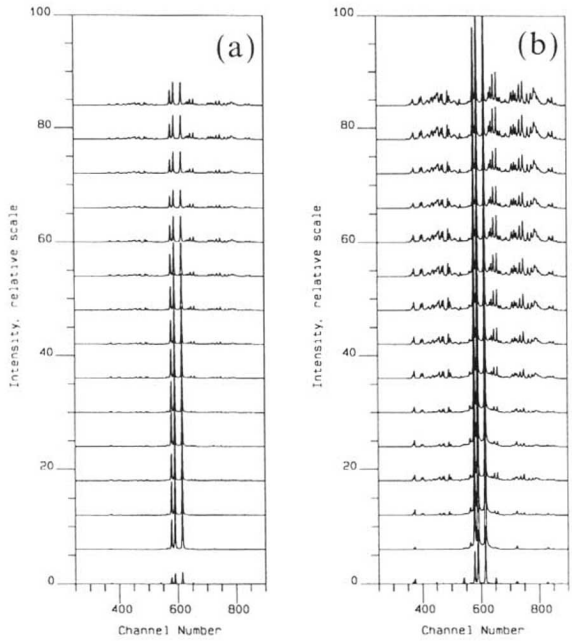

Fig. 1. Gated spectral intensities from laser-produced plasma plumes from a fixed area on the surface of a galvanized steel specimen which have been repetitively excited by laser pulses. Each of the 15 emission spectra are separated by 10 laser excitations, the 1st excitation being at the bottom and the 140th appearing at the top. The sequence corresponds to 15 depths from the surface. The spectra on the left-hand side (a) are the same as those shown on the right (b) but are displayed compressed by a factor of five in intensity scale from those on the right. The three zinc emission lines in the middle can be followed to see their decline in intensity with increasing depth (a), while the iron lines are seen to emerge more strongly as the number of laser excitations increases (b).

The galvanized steel specimen was then subjected to more than 650 laser excitations at a fixed laser power density. As the excitation was continued, the spectral emission showed a gradual transition from a makeup of overwhelming zinc domination to another where iron dominated. This is shown in Fig. 1: 15 successive emission spectra separated by 10 laser excitations are displayed at two intensity resolutions. To help ameliorate the difficulty in discerning the two sets of elemental emission lines arising from the large disparity between the atomic transition probabilities of zinc and iron, the same spectra are shown on two different intensity scales. Figure 1b is five times more sensitive than Fig. 1a. The earliest emission lines are nearly entirely due to zinc, and the new features seen later on are due to iron. Figure 2 shows that the zinc concentration decreases with depth, while the iron concentration increases. The presence of zinc, however, persists deep into the bulk.

The measured mass loss as a function of the number of laser excitations is shown in Fig. 3. The mass loss per laser excitation, as shown, is an average of the total mass loss during 10 successive laser excitations. The specimen is removed from the specimen holder of the chamber, weighed, and repositioned after every 10 laser excitations. Care was taken to

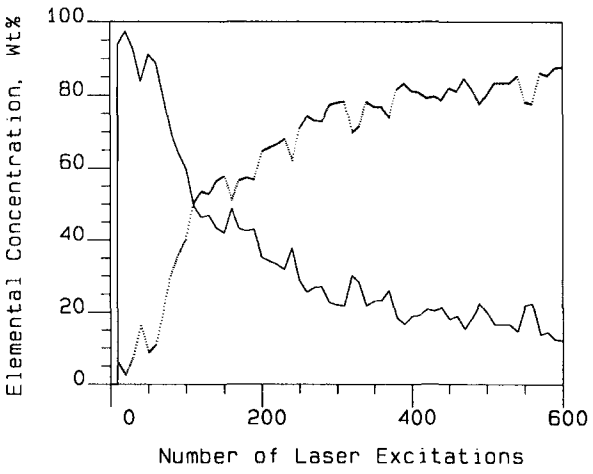

Fig. 2. Weight percentage for zinc (solid line) and iron (dotted line) in the surface layers of the galvanized steel specimen as a function of the number of laser excitations. The results shown here are deduced from the gated spectral intensities in Fig. 1. The concentration values were tabulated at every tenth excitation and then linearly interpolated between successive points. The procedure is explained in the text.

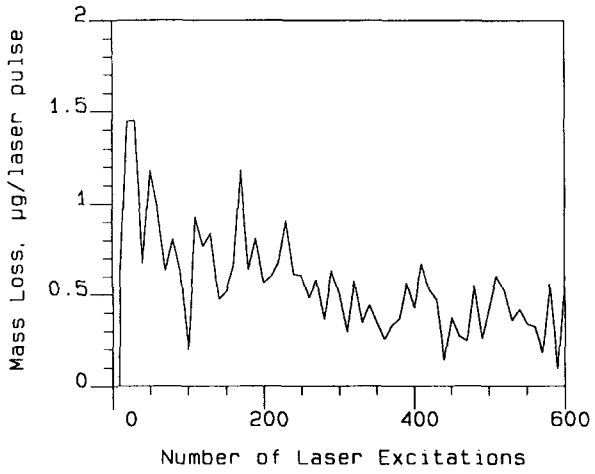

Fig. 3. The measured mass loss per laser excitation as a function of the number of successive laser excitations. The specimen was weighed after every 10 laser excitations with a digital microbalance of 0.1-μg resolution. The measurement error is due primarily to the zero drifts of the microbalance, and the maximum possible error is $\leqslant 0.2$ μg throughout. The composition inhomogeneity within the surface layers contributes significantly to the scatter.

preserve the orientation of the specimen with respect to the polarization axis of the laser beam. The gated intensity emission spectrum was taken at each of the first 50 laser excitations and at the last of every 10 additional excitations thereafter. The measured mass loss values are shown linearly interpolated between successive measurements in the display of Fig. 3.

The mean mass loss averaged over the entire 650 laser excitations is 0.61 μg per laser excitation. At the mean mass density of 7.59 $g \cdot cm^{-3}$, this translates to a mean thickness of the surface layer removed per laser excitation of 24.9 nm. It is clear that the mass loss starts off small at the start of the laser excitation, rapidly rises to the highest value over the next few laser excitations, and decreases slowly at subsequent laser excitations. The scatter in the data is due partly to the zero drifts in the microbalance and partly to the composition inhomogeneity over the focal area at different depths. The upper bounds to the measurement error in the mass loss due to the microbalance drift can be set at ± 0.2 μg but the actual point-to-point measurement error is usually less than these values. The zero-drift contributions to the measurement error can, in principle, be reduced if more time is allowed for the microbalance to stabilize. However, to offset the more complicated process of atmospheric modifications of the freshly

exposed specimen surface, we chose to limit the total time allotted for the entire sequence of 10 laser excitations, spectrum acquisition, and specimen weighing to 2 min. At each weighing, the microbalance has had a fixed resettling time after each preceding weighing session.

4. SPECTROSCOPIC DETERMINATION OF THE MASS LOSS

We now turn to the question of how to determine the mass loss by purely spectroscopic means and thereby execute the thermal diffusivity measurement without making any physical contact with the specimen either by a transducer or through some weighing process. The gated intensity spectrum such as those shown in Fig. 1 contains the quantitative information of the total mass of the plasma which has been created out of the plume driven out of the specimen surface by laser excitation.

The conversion of the spectrum into mass content for a multielement alloy specimen, however, requires an appropriate rescaling for different elemental emission line intensities according to their respective atomic transition probabilities. This is because a spectral emission line intensity from an elemental species present in a plasma in local thermodynamic equilibrium is a product of the abundance of the species and the atomic transition probability between the conjugate pair of excited electronic states. The detected gated intensity results from threefold integration of the equation of radiative transfer, which governs the local spectral intensity within the plasma, first along the line of sight, next over the line profile, and finally, in time for the lifetime of the plasma afterglow [5].

The rescaling of elemental emission line intensities has been carried out for the spectra taken from the galvanized steel specimen. First, the emission spectrum from a pure zinc specimen was taken after the surface had been cleaned by several laser excitations under conditions identical to those for the galvanized steel specimen. Similarly, the emission spectrum was obtained for a pure iron specimen. After correcting for the difference in the optical reflectance of the two pure elemental specimens, the sum of the intensities of a group of the most prominent emission lines of zinc is compared with that for a group of several prominent iron lines. The ratio of the two sum intensities is used as the scaling constant between the two elements for the spectral intensity to mass conversion.

Figure 4 shows the mass loss as derived from the emission spectra, each taken at the end of each 10-excitation segment, as a function of the number of laser excitations. The result compares very well with that of directly measured mass losses, shown in Fig. 3, for the entire sequence of laser excitations, except for the earliest sequence. The outermost layers of the galvanized steel surface has a more complex makeup, including oxides,

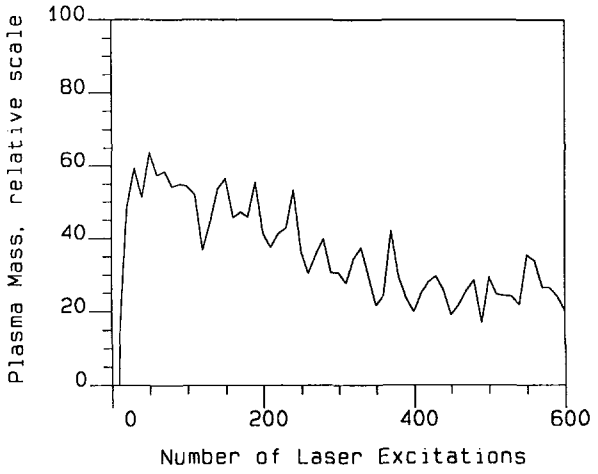

Fig. 4. The total mass contained in the plasma plume as a function of the number of laser excitations. This mass is determined from the gated spectral intensities in Fig. 1 by first determining the scaling constant between the sum intensity of a group of zinc emission lines and that for a group of iron lines. This spectrum-derived mass is to be compared with the mass losses determined by weighing as shown in Fig. 3.

and had not been characterized enough to be incorporated into the spectroscopic method for mass loss determination.

The spectrum-derived mass loss also provides the composition of the matter driven out of the specimen surface. If the same matter is assumed to be compact while existing in condensed phase on the surface, the effective molar weight, specific heat, and the mass density of the layer can be calculated as a function of the number of laser excitations. It is then just a short step to full calculation of the thermal diffusivity as a function of depth from the outermost surface of the specimen. The purely spectrum-derived thermal diffusivity is shown in Fig. 5 in a relative form. Given that the mass loss scales with the thermal diffusivity according to Eq. (1) and that the mass loss has approached an asymptotic value near the end of the long series of laser excitations, we conclude that the bulk thermal diffusivity of the specimen deep beneath the surface layer is given by the average of the measured mass losses from the last 50 laser excitations. The relative thermal diffusivity is then calculated from the depth-resolved mass loss in reference to the bulk mass loss through Eq. (1). The thermal diffusivity profile at the surface region of the galvanized steel specimen is thus found over the first 16.2 μm depth from the free surface.

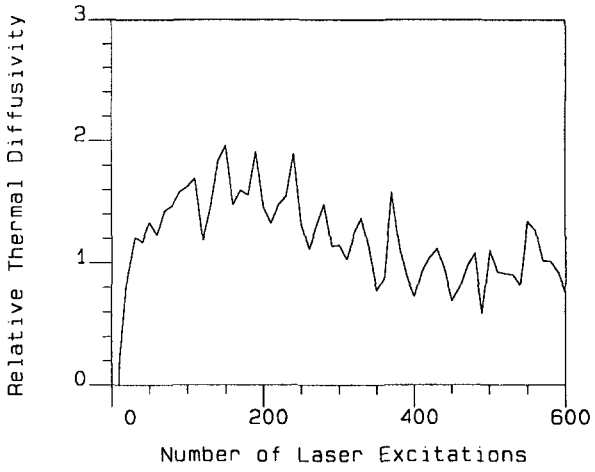

Fig. 5. The relative thermal diffusivity of the galvanized steel specimen as a function of the number of laser excitations, as found from the gated spectral intensities. The diffusivity is referenced to the average of the thermal diffusivity values based on the spectroscopically determined mass losses from the last 50 laser excitations of the series. This reference bulk layer lies at a depth of approximately 60 μm beneath the free surface of the specimen. The mass loss measurement shows that an asymptotic value for the thermal diffusivity has been reached at this depth.

5. CONCLUSIONS

In this paper, a new systematic method is presented for depth-resolved determination of the thermal diffusivity of the surface region of a bulk specimen. Furthermore, an *in situ*, noncontact method for determining the mass loss due to pulsed laser excitation of the surface is described for the first time. The method is based entirely on quantitative spectroscopy. Together, the thermophysical property is completely obtained by purely spectroscopic means. As such, this is of considerable practical importance because it makes it possible to carry out measurements under conditions not accessible to alternative methods. Examples are materials at high temperatures such as in pyrometallurgical processes or hazardous materials or those in hazardous environments. Of much more basic importance is in the fact that the all-spectroscopic method makes it possible to make measurements of thermophysical properties simultaneously with the local elemental composition of the condensed-phase specimens. This will make it possible to gain an understanding, on a first principle basis, of the relationship of the thermophysical properties to the composition of a given material.

The layer-to-layer variations seen in the mass loss, composition, and the thermal diffusivity are due to a large extent to the composition inhomogeneities over the focal area as well as over the submicron depth scales and the resultant changes in local thermal diffusivity. There are no other comparable measurements available for comparison at the present time.

This investigation has been extended to much higher ambient gas densities, exceeding 100 atm at room temperature. Details will be presented in later publications.

REFERENCES

1. Y. W. Kim, *High Temp. Sci.* **26**:57 (1990).
2. Y. W. Kim and C. S. Park, *Int. J. Thermophys.* **17**:713 (1996).
3. Y. W. Kim and C. S. Park, *Int. J. Thermophys.* **17**:1125 (1996).
4. *American Institute of Physics Handbook*, 3rd ed. (McGraw–Hill, New York, 1972); *CRC Handbook of Chemistry and Physics*, 75th ed. (CRC Press, Boca Raton, FL, 1994).
5. Y. W. Kim, in *Laser-Induced Plasmas and Applications*, L. J. Radziemski and D. A. Cremers, eds. (Marcell Dekker, New York, 1989), Chap. 8.